TaD27-B gene controls the tiller number in hexaploid wheat

Bin Zhao[1,†], Ting Ting Wu[1,†], Shan Shan Ma[1], Deng Ji Jiang[1], Xiao Min Bie[1], Na Sui[2] (iD), Xian Sheng Zhang[1,*] and Fang Wang[1,*] (iD)

[1]*State Key Laboratory of Crop Biology, College of Life Sciences, Shandong Agricultural University, Taian, Shandong, China*

[2]*Shandong Provincial Key Laboratory of Plant Stress, College of Life Science, Shandong Normal University, Jinan, China*

Summary

Tillering is a significant agronomic trait in wheat which shapes plant architecture and yield. Strigolactones (SLs) function in inhibiting axillary bud outgrowth. The roles of SLs in the regulation of bud outgrowth have been described in model plant species, including rice and *Arabidopsis*. However, the role of SLs genes in wheat remains elusive due to the size and complexity of the wheat genomes. In this study, *TaD27* genes in wheat, orthologs of rice *D27* encoding an enzyme involved in SLs biosynthesis, were identified. *TaD27*-RNAi wheat plants had more tillers, and *TaD27-B*-OE wheat plants had fewer tillers. Germination bioassay of *Orobanche* confirmed the SLs was deficient in *TaD27*-RNAi and excessive in *TaD27-B*-OE wheat plants. Moreover, application of exogenous GR24 or TIS108 could mediate the axillary bud outgrowth of *TaD27*-RNAi and *TaD27-B*-OE in the hydroponic culture, suggesting that *TaD27-B* plays critical roles in regulating wheat tiller number by participating in SLs biosynthesis. Unlike rice *D27*, plant height was not affected in the transgenic wheat plants. Transcription and gene coexpression network analysis showed that a number of genes are involved in the SLs signalling pathway and axillary bud development. Our results indicate that *TaD27-B* is a key factor in the regulation of tiller number in wheat.

Introduction

Plant architecture, a significantly agronomic trait shaped by shoot branching (tillering), is one of the critical factors that determine grain yield. In higher plant, the plant architecture consists of main stem and shoot branches, which is produced by shoot apical meristem (SAM) and axillary meristems (AMs), respectively (Mcsteen and Leyser, 2005). Shoot branching is normally divided into two developmental steps: the generation of an AM in each leaf axil and consequent outward growth. After generation, axillary buds may either remain dormant or produce a lateral branch in response to the different signals mediated by plant hormones (Mcsteen and Leyser, 2005; Shimizu-Sato and Mori, 2001).

Shoot branching is regulated by multiple phytohormones. SLs were recently identified as endogenous plant hormones, and it was reported that SLs can inhibit the outgrowth of axillary bud (Umehara *et al.*, 2008). The D27/AtD27, CCD7 and CCD8 proteins, which were localized in the plastid, participate in the biosynthesis of SLs. The carotenoid isomerase (D27/AtD27) is in charge of transforming all-trans-b-carotene into 9-cis-b-carotene (Lin *et al.*, 2009; Waters *et al.*, 2012). CCD7 can cleave 9-cis-b-carotene into 9-cis-b-apo-10′-carotenal, and CCD8 can produce the carlactone, which is the precursor of SLs (Alder and Al-Babili, 2012). Then, the cytochrome P450 oxygenase MAX1 converts carlactones into SLs (Booker *et al.*, 2005).

The genes involved in the biosynthesis or signal transduction of SLs are required for regulating the axillary bud outgrowth and shoot branching. In *Arabidopsis* and rice, *D27* gene encodes an iron-containing chloroplast protein; *d27* mutant plants show defective SLs biosynthesis and exhibit extensive outgrowth of

axillary buds (Lin *et al.*, 2009; Waters *et al.*, 2012). Rice *HIGH-TILLERING DWARF1* (*HTD1*), encoding CCD7, can inhibit the outgrowth of axillary buds and the tillering in rice (Zou *et al.*, 2005). Rice *D10* encoding CCD8 is an ortholog of *RMS1/MAX4/DAD1* in *Arabidopsis*. The expression of *OsPINs* was decreased in shoot nodes, which resulted in the capacity reduction of auxin transport in *D10*-RNAi-transgenic plants (Arite *et al.*, 2010). The branched phenotype and the effects of *MAX1* mutation can be rescued by *OsMAX1a* and *OsMAX1e* in *Arabidopsis*. In addition, the expression of *OsMAX1a* and *OsMAX1e* is sensitive to P deficiency in rice (Wang *et al.*, 2015). DWARF53 (D53) acts as the degradation of the SLs signalling repressor, which is mediated by the receptor complex in rice and *Arabidopsis* (Jiang *et al.*, 2013; Soundappan *et al.*, 2015; Zhou *et al.*, 2013). *OsMADS57*, encoding a MADS-box transcription factor (TF), is expressed predominantly in the SAM and axillary buds. *OsMADS57* can directly inhibit the expression of *D14* and be targeted by miR444a. It was revealed that *OsMADS57* can promote the outgrowth of axillary buds and tillering via SLs signalling. The tiller numbers of *OsMADS57* overexpression and RNAi-transgenic plants were significantly changed compared with those in the wild-type plants (Guo *et al.*, 2013).

Tillering is a significant agronomic trait of wheat, which determines plant architecture and spike number. So far, a number of several tillering mutant loci were identified in barley (*Hordeum vulgare* L.), such as *uniculm2* (*cul2*; Babb and Muehlbauer, 2003), *absent lower laterals* (*als*; Dabbert *et al.*, 2009), *low number of tillers1* (*lnt1*; Dabbert *et al.*, 2010) and *uniculme4* (*cul4*; Tavakol *et al.*, 2015), which fail to produce tillers or have the fewer number of tillers owing to weakened axillary bud outgrowth. In

additio*n, Many-noded dwarf* (*Mnd*) gene was rapidly identified by mapping-by-sequencing in barley (Mascher *et al.*, 2014). The vegetative shoot branches can develop from lateral meristems, which lead to increased tiller number in *mnd* mutants.

Wheat (*Triticum aestivum* L.) is one of the most valuable cereal crops. SLs are required for shoot branching, and thus, the yield can be increased by the manipulation of SLs biosynthesis (Conn *et al.*, 2015; Lópezráez *et al.*, 2010). The main steps of SLs biosynthesis and signalling were elucidated by the studies of SLs-deficient and perception mutants (Albabili and Bouwmeester, 2015; Jia *et al.*, 2017; Waters *et al.*, 2017). However, there is little information about the key regulatory genes for the biosynthesis and transport of SLs, and the roles of these genes functioning in tillering remain unknown in wheat. In this study, three *TaD27* genes were identified and characterized in wheat, and it was demonstrated that *TaD27*-RNAi wheat plants had more tillers and *TaD27-B*-OE wheat plants had fewer tillers, suggesting that the wheat *TaD27-B* gene plays critical roles in regulating the wheat tiller number. By comparing the transcriptomes of wild-type and *TaD27*-RNAi axillary bud primordia, many genes involved in the SLs signalling pathway and axillary bud development were identified in wheat, confirming the SLs signalling pathway mediates axillary bud development. Further functional analysis of the identified genes might help us understand the mechanism of tiller regulation in wheat.

Results

Identification of *TaD27* genes in hexaploid wheat

D27, an iron-containing protein, participates in SLs biosynthesis and regulates axillary bud outgrowth through the MAX/RMS/D pathway in rice (Lin *et al.*, 2009). To investigate the regulatory role of SLs during shoot branching in wheat, we conducted a BLAST against IWGSC Survey Sequence Assemblies using the CDS sequence of *D27* (Os11g0587000) in rice as a seed sequence. Three highly conserved full sequences (TRIAE_CS42_7AL_TGAC-v1_557393_AA1780700, TRIAE_CS42_7BL_TGACv1_577741_AA1882380 and TRIAE_CS42_7DL_TGACv1_603164_AA1977390) were obtained, indicating that wheat *D27* genes have three homologous loci (annotated in *TaD27-A*, *TaD27-B* and *TaD27-D* in this study) on the A, B and D chromosomes, respectively. Primers were designed according to the assembled sequences to amplify the genomes and cDNA samples from wheat line Kenong 199. Their genomic sequence lengths were 2066, 2058 and 2081 bp, and they encoded putative products of 279, 280 and 280 amino acids, respectively. The TaD27 proteins were highly conserved with D27 proteins in *Arabidopsis* and rice, suggesting that they were orthologs of D27 proteins (Figure S1).

To investigate the evolutionary relationships of *TaD27* genes, a phylogenetic tree of D27 proteins from various plant species was constructed. The dendrogram showed that the TaD27 proteins were most closely related to D27 proteins in *Aegilops tauschii*, *H. vulgare*, *Brachypodium distachyon* and *Oryza sativa* ssp. *japonica* (Figure 1). To understand the structural features of the *D27* genes, the numbers and positions of exons and introns of each *D27* gene were determined by the comparison of the transcript sequences and the corresponding genomic DNA sequences via GSDS2.0 (Gene Structure Display Server) website (http://gsds.cbi.pku.edu.cn). The results revealed that all of them contain seven exons and six introns, implying strong conservation of gene structure during evolution (Figure 1). Thus, it confirmed that we have identified three *TaD27* genes in hexaploid wheat.

Expression patterns of *TaD27*s and subcellular localization of TaD27-B protein

To explore the potential roles of the *TaD27*s in wheat growth and development, the expression patterns of TaD27s were analysed in wheat. The results showed that the *TaD27*s were expressed in all the organs tested, and the expression level was highest detected in leaves compared with other organs (Figure 2a). Because the three TaD27s had extremely high similarities in their amino acid sequences and *TaD27-B* had higher expression in leaves and axillary buds, *TaD27-B* was selected for further functional analysis.

The expression patterns of the *TaD27*-B were further examined using mRNA *in situ* hybridization. The results showed that *TaD27-B* was strongly expressed in the AMs although their expression was detected in other tissues, such as the young leaves, SAM and spikes, indicating that *TaD27-B* might play a role in the development of tiller in wheat (Figure 2b).

To determine the subcellular localization of the TaD27-B, the *35S*::*TaD27-B-GFP* construct was introduced into *Arabidopsis* leaf protoplasts. As shown in Figure 2c, the fluorescence was ubiquitous in the control of protoplast cells, whereas the TaD27-B-GFP fusion protein was predominantly localized in the chloroplast (Figure 2c). Thus, TaD27-B appeared to be located in chloroplasts of wheat.

TaD27-B is a functional ortholog of *D27* in *Arabidopsis*

To verify the biological function of the *TaD27-B*, we first introduced the *35S*::*TaD27-B* vector into *Arabidopsis Atd27* mutant plants (CS761234). Three independent transgenic lines (*35S*::*TaD27*-11, *35S*::*TaD27*-13 and *35S*::*TaD27*-20) were selected for phenotypic analysis. The result showed that the expression levels of *TaD27-B* were elevated in all three transgenic lines. Moreover, the expression level of *TaD27-B* in *Atd27* reduced the average number of branches and led to a branching phenotype similar to that of wild-type *Arabidopsis* plants, indicating that the expression of *TaD27-B* in *Atd27* plants almost completely restored the phenotype back to that of the wild type (Figure S2). Thus, *TaD27-B* is a functional ortholog of *D27* in *Arabidopsis*.

Phenotypes of *TaD27s*-transgenic wheat lines

To determine the potential functions of the *TaD27*s in wheat, *TaD27-B* knock-down lines were generated through RNA interference in wheat. We constructed an RNAi vector (*TaD27*-RNAi) and transformed this construct into hexaploid wheat (cv. Kenong199). In total, 16 *TaD27*-RNAi T0-transgenic plants were confirmed. Three T3 lines (48#, 50# and 55#) were selected for further analysis (Figure S3).

To investigate the vegetative and reproductive development phenotypes, the *TaD27*-RNAi-transgenic wheat lines were sowed under field conditions. We characterized the biological roles of the *TaD27* genes in the regulation of wheat plant architecture in detail. It is found that the most significant aspect of the phenotypes of the *TaD27*-RNAi plants was the enhanced tillering. Compared with the wild-type KN199, more visible axillary buds were observed in *TaD27*-RNAi seedlings at the vernalization stage (Zadoks scale of growth: Z26; Figure 3a), indicating that decreased expression of *TaD27*s led to easier and earlier production of lateral branches. After turning green in spring, the *TaD27*-RNAi-transgenic lines had more tillers than the wild-type KN199 and showed a bushy phenotype to some extent at
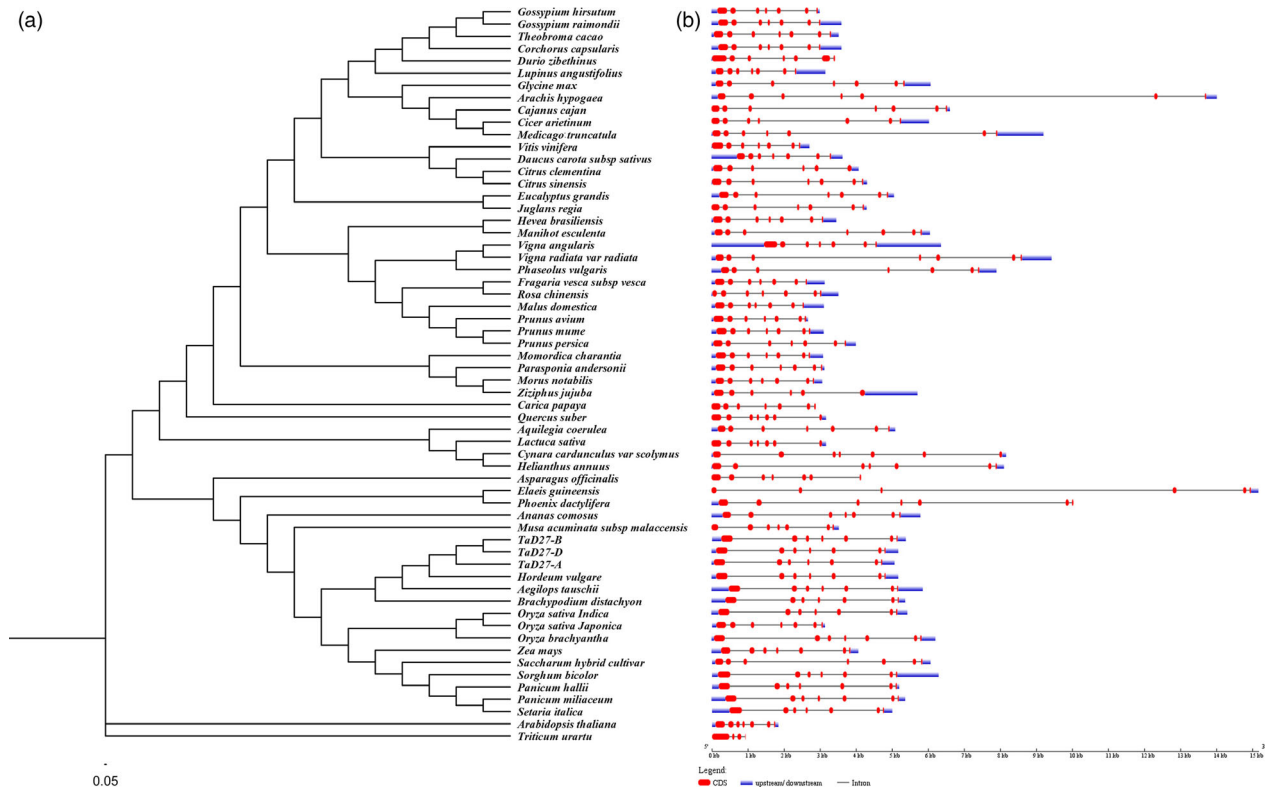
Figure 1 Phylogenetic relationships and gene structures of the TaD27s and other D27 proteins. (a) Phylogenetic tree of D27s constructed from a complete alignment of 60 D27 protein sequences by the neighbour-joining method with 1000 bootstrap replicates using MEGA 7.0. (b) Exon/intron structures in the CDSs of *D27* genes, exons are represented by red boxes, and introns are represented by black lines. The sizes of exons and introns can be estimated using the scale at the bottom.

two developmental stages including the heading stage (Z33) and the mature stages (Z85) as shown in Figure 3. The statistical analyses showed that the decreased expression of *TaD27s*, especially *TaD27-B*, caused an obvious increase in tillers in the *TaD27*-RNAi lines compared with the wild type (Figure 3d–f,h). In rice, *d27* mutant plants showed an increased tillering and severe dwarf phenotype at the mature stage (Lin *et al*., 2009). However, there were no conspicuous differences in plant height between the wild-type and *TaD27*-RNAi wheat plants (Figure 3g).

To further understand the function of *TaD27-B* in wheat tillering, we also developed overexpression transgenic lines with an *ubi*::*TaD27-B* vector. We obtained 26 independent *TaD27-B*-overexpressing (*TaD27-B*-OE) transgenic lines. Three *TaD27-B*-OE lines (31#, 59# and 92#) were selected for further analysis. The expression level of *TaD27-B* was significantly increased and much higher in the *TaD27-B*-OE lines than the wild-type KN199. Compared with the wild-type KN199, three lines displayed reduced tiller numbers (decreased by 17%–50% in different transgenic lines) at different developmental stages (Figure 4). These results demonstrated that overexpression of *TaD27-B* suppresses tillering in wheat. The expression abundance of *TaD27-A* and *TaD27-D* was also been detected in *TaD27-B*-OE lines. The result showed that their expression levels were higher in the *TaD27-B*-OE lines than in the wild-type KN199. It is likely that there is a feedback regulation among *TaD27-A*, *TaD27-B* and *TaD27-D* (Figure 4h).

The tiller develops from an axillary bud, and the axillary bud number is rapidly increased from the three-leaf stage to the

jointing stage, reaching a maximum before subsequently decreasing. If its length is over 2 cm, we consider the axillary bud as a visible tiller. To identify the effect of *TaD27-B* on axillary number, the axillary bud number and the proportion of visible tiller were counted at the jointing stage (Z32). There were total 32 ± 2 axillary buds, and the proportion of visible tiller was $56.7\% \pm 1.5\%$ in *TaD27*-RNAi plants. In contrast, the axillary buds were 15 ± 3, and the proportion of visible tiller was $51.2\% \pm 2.4\%$ in *TaD27-B*-OE plants. In control plants, the axillary bud number was 24 ± 2, and the proportion of visible tiller was $53.8\% \pm 1.9\%$. The results indicate that *TaD27-B* affects axillary bud number and thus ultimately affect the tiller number.

TaD27-B functions in SLs biosynthesis

In *Arabidopsis* and rice, mutation of *D27* resulted in reduced SLs production and increased branching (Lin *et al*., 2009; Waters *et al*., 2012). Decreased *TaD27s* expression in wheat also increased branching (Figure 3). Based on the tillering phenotype, we predicted that the SLs levels might be significantly deficient in *TaD27*-RNAi plants and excessive in *TaD27-B*-OE plants. To determine the endogenous levels of SLs, the germination assay was carried out to estimate the ability of root exudates of *TaD27*-RNAi, *TaD27-B*-OE and wild-type plants (Z12) to stimulate germination using seeds of the *Orobanche*. The results revealed that the ability of root exudates to stimulate germination was severely reduced in *TaD27*-RNAi plants and significantly enhanced in *TaD27-B*-OE plants compared to that in wild-type plants
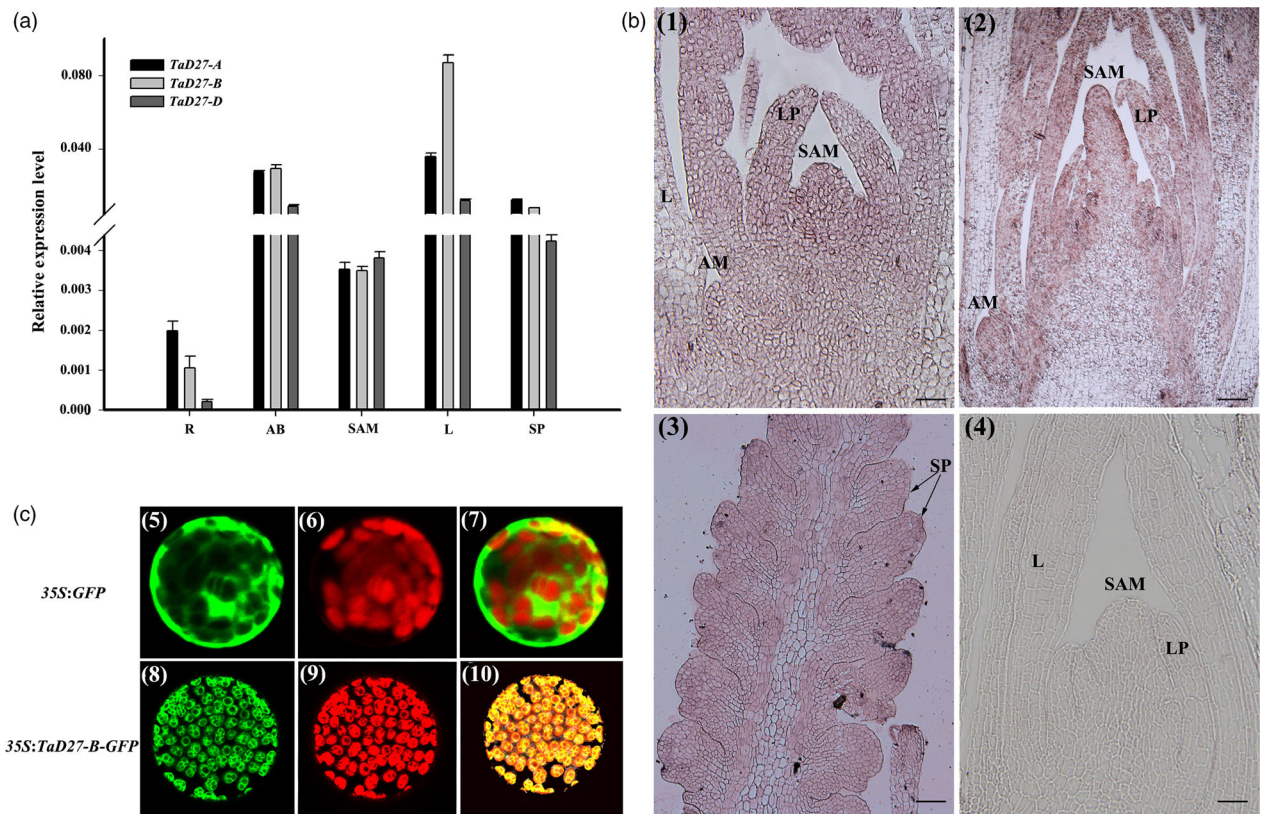
Figure 2 Expression patterns of *TaD27*s and subcellular localization of the TaD27-B protein. (a) Expression patterns of *TaD27*s in wheat. R, roots (Z12); AB, axillary buds (Z15); SAM, shoot apical meristem (Z13); L, leaves (Z13); SP, spikelet primordia (Z17). (b) *In situ* hybridization analysis of *TaD27-B*. (1) Longitudinal section of the shoot apex at the single ridge stage showing axillary buds (Z13). (2) Longitudinal section of the shoot apex at double ridge stage showing axillary buds (Z15). (3) Longitudinal section of a spike (Z17). (4) Sense probe control; AM, axillary meristem, SP: spike primordium. Bars = 100 μm. (c) Subcellular localization of the TaD27-B protein. (5–7) The pROKII control vector is located in the cell membrane and cytoplasm; (8–10) 35S::TaD27-B-GFP is located in the chloroplasts. Bars = 5 μm.

(Figure 5a), confirming that *TaD27-B* plays a critical role in SLs biosynthesis in wheat.

Next, we found that the axillary buds of 3-week-old *TaD27*-RNAi seedlings (Z12) were markedly enlarged compared with those in the wild type. By applying 5.0 μM GR24, a synthetic SLs analog (Mangnus *et al.*, 1992), to *TaD27*-RNAi seedlings in the hydroponic culture, it was shown that exogenous application of GR24 fully inhibited the axillary bud outgrowth of 3-week-old *TaD27*-RNAi seedlings (Figure 5b). Moreover, the axillary buds of 3-week-old *TaD27-B*-OE seedlings (Z12) were inhibited compared with those in the wild type. Whereas, by applying 3.0 μM TIS108, an azole-type SLs biosynthesis inhibitor (Ito *et al.*, 2011), the development of the axillary buds was restored in *TaD27-B*-OE seedlings (Figure 5c). These results confirmed TaD27-B functions in SLs biosynthesis in wheat.

RNA-seq analysis identified possible downstream regulatory genes for tillering

To further dissect the molecular basis of tiller generation, we performed an RNA-seq analysis of 3-week-old *TaD27*-RNAi axillary bud primordia (Z14–Z15). The axillary buds of the wild-type KN199 at the same development stage were used as the control (Table S3). A total of 4947 differentially expressed genes (DEGs) were obtained using a fold change of 2 and FDR < 0.05. Among them, 4124 genes were expressed at a low level and 823

genes were highly expressed in *TaD27*-RNAi compared with the wild type (Table S4).

In rice and *Arabidopsis*, plastid-localized enzymes encoded by *D27*, *D10/MAX4*, and *D17/MAX3* play roles in catalysing the formation of carlactone, which is further catalysed by cytochrome P450 to generate SLs (Zhang *et al.*, 2014). *D14*, *D3* and *D53* were required for the regulation of the axillary bud outgrowth in rice. The *TaD27*s transcript levels were significantly reduced in *TaD27*-RNAi plant (Figure 3h). The RNA-seq and qRT-PCR analysis showed that the expression levels of *TaMAX1*, *TaD14* and *TaD53* genes were also markedly down-regulated (Figure 6a; Table S4). This suggests that SLs synthesis and signal transduction were suppressed in *TaD27*-RNAi-transgenic plants.

As shown in Figure 6b, the analysis of the DEGs suggests that multiple processes were affected in *TaD27*-RNAi axillary buds. It was worth noting that the GO term catalytic activity was significantly enriched, suggesting that the expression levels of genes involved in the catalytic process were affected by knock-down of *TaD27*s. The genes for diverse processes were also enriched including metabolic processes, cellular processes, biological regulation, cell parts, single-organism processes and binding, implying that the development of axillary bud might be a consequence of multiple biological processes. To verify the reliability of our RNA-seq data, 12 DEGs were randomly chosen and detected by qRT-
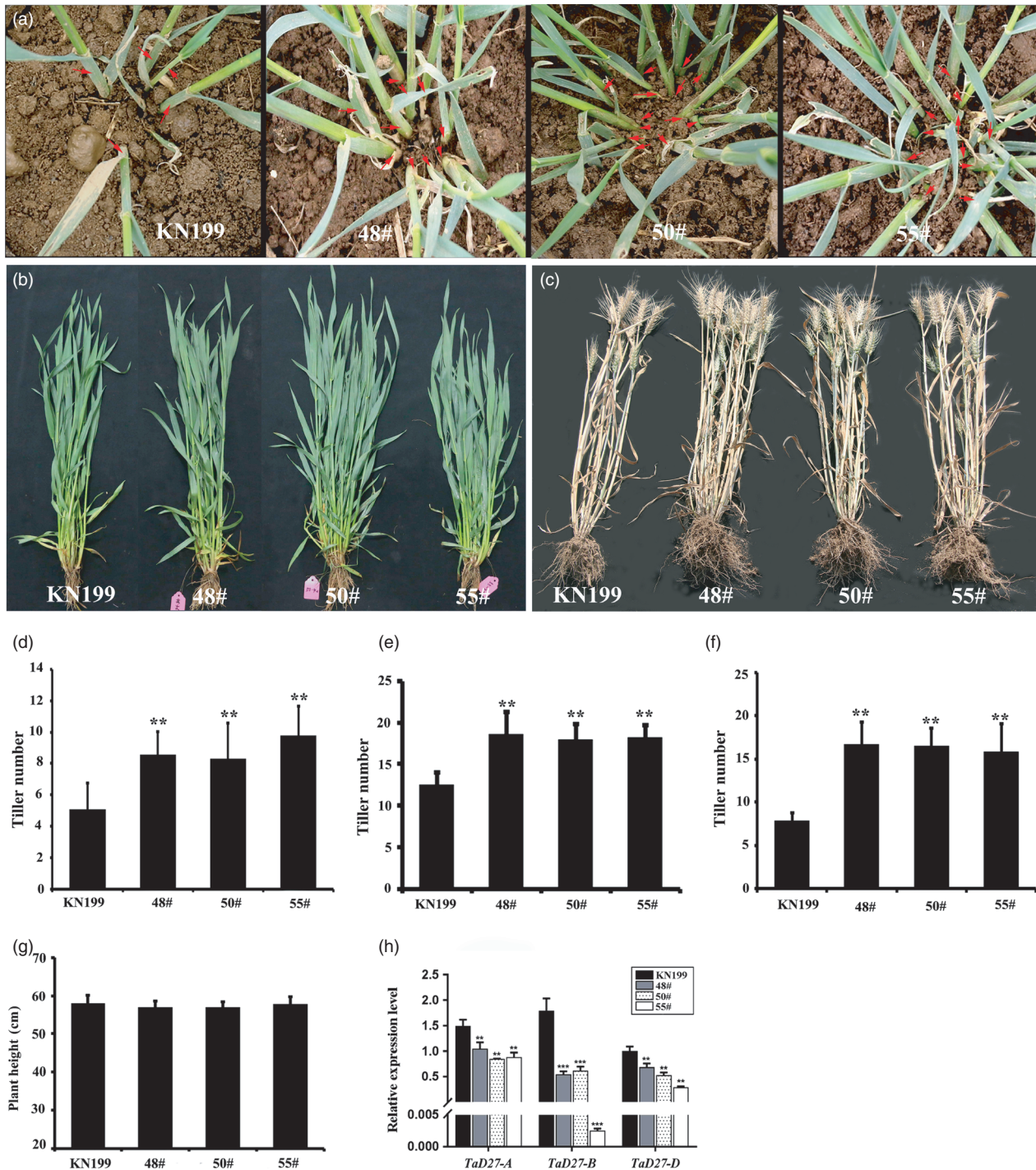
Figure 3 Morphological characters of *TaD27*-RNAi wheat plants. (a–c) Appearance of visible tiller buds in wild-type KN199 and *TaD27*-RNAi seedlings at the vernalization (a), jointing (b) and mature (c) stages. Red arrows indicate the positions of tiller buds. (d-f) Column diagrams showing statistical analyses of the tiller numbers of the wild-type KN199 and three independent transgenic lines at the vernalization (d), jointing (e) and mature (f) stages. (*n* = 30). (g) Column diagram showing statistical analysis of plant height in the wild-type KN199 and three independent transgenic lines. (h) The expression of *TaD27*s in KN199, 48#, 50# and 55# plants in the seedling stage. Single, double and three asterisks represent significant differences between the wild-type and T3 generation *TaD27*-RNAi-transgenic plants in Student's *t*-test at *P* < 0.01.

PCR. It is shown the relative expression patterns of 12 DEGs were generally consistent with our RNA-seq data, confirming our data are reliable (Figure S5).

To further understand the putative active biological pathways, the identified DEGs were mapped to the KEGG database. The top

20 overrepresented pathways are displayed in Figure 6c. Besides metabolic pathways and the biosynthesis of secondary metabolites, hormone signal processes were enriched in the DEGs, suggesting that hormones play a significant role in tiller development in wheat. SLs are involved in the regulation of various
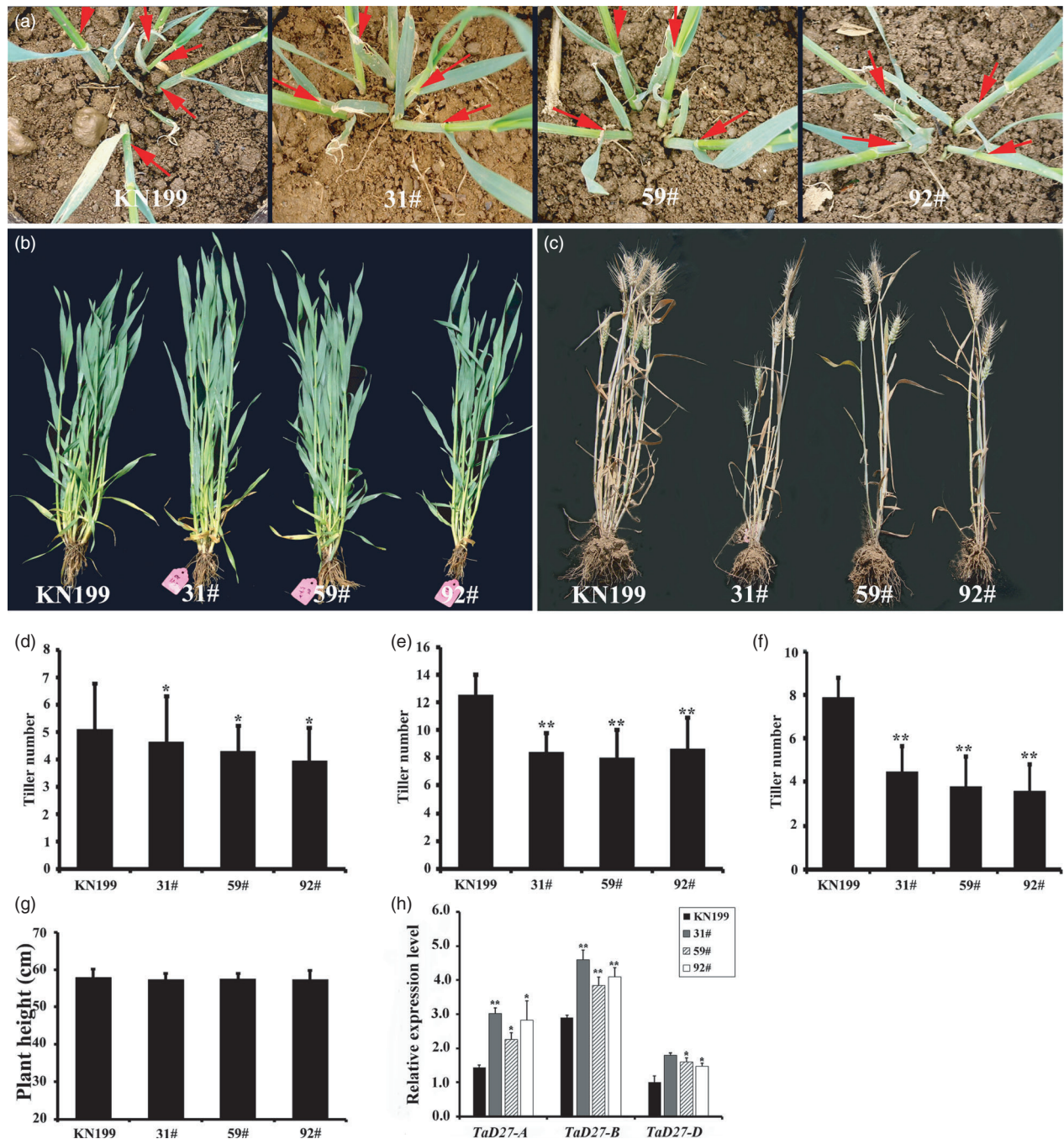
Figure 4 Morphological characters of *TaD27-B*-OE wheat plants. (a–c) Appearance of visible tiller buds in wild-type KN199 and *TaD27-B*-OE seedlings at the vernalization (a), jointing (b) and mature stages (c). Red arrows indicate the positions of tiller buds. (d-f) Column diagrams showing statistical analyses of the tiller number of the wild-type KN199 and three independent transgenic lines at the vernalization (d), jointing (e) and mature (f) stages. ($n \geq 30$). (g) Column diagram showing statistical analysis of plant height in the wild-type KN199 and three independent transgenic lines. (h) The expression of *TaD27s* in KN199, 31#, 59# and 92# plants in the seedling stage. Single and double asterisks represent significant differences between wild-type and T3 generation *TaD27-B*-OE transgenic plants in Student's *t*-test at $P < 0.01$.

plant developmental processes, especially in crosstalk with other phytohormones, such as auxin (Albabili and Bouwmeester, 2015).

A number of DEGs involved in auxin synthesis and signal processes were identified (Figure 7a). Increasing evidence has revealed interaction between auxin and SLs in plants. In our data, the auxin biosynthetic *TAA/YUC* genes were present among the DEGs. Furthermore, three *ALDEHYDE DEHYDROGENASE* (*ALDH*)

genes, five *INDOLE-3-ACETALDEHYDE OXIDASE* 3 (*AO*) genes and four *gatA* genes were auxin biosynthetic genes in KEGG (pathway 00380) (Figure 7a). A number of genes involved in auxin signalling (pathway 04075) were also identified. *AUXIN/INDOLE ACETIC ACID* (*IAA*) and *SMALL AUXIN UP RNA* (*SAUR*) family genes belong to early auxin-responsive genes (Hagen and Guilfoyle, 2002), and the DEGs analysis revealed that most of the
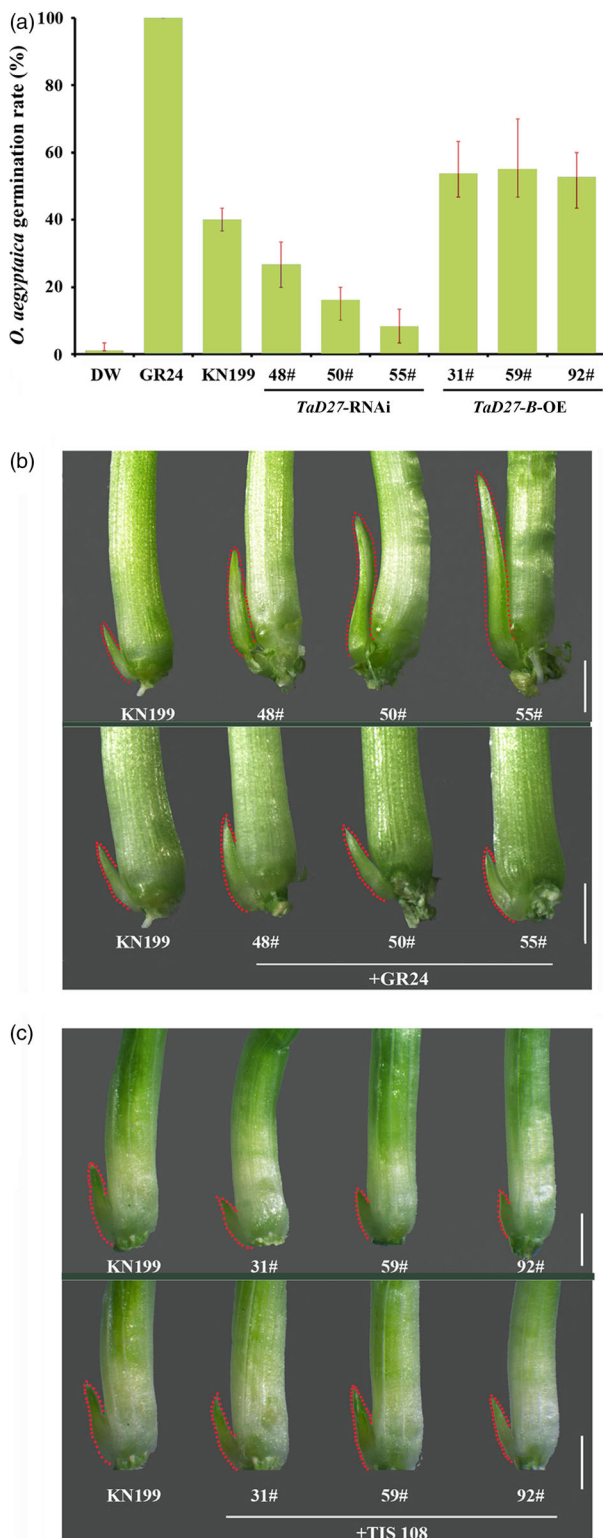
Figure 5 (a) Germination rates of *Orobanche* seeds at 10 days after treatment with deionized water (DW), GR24 and root extracts of wild-type control (KN199), *TaD27*-RNAi and *TaD27-B*-OE lines. DW and GR24 are the negative and positive controls, respectively. (*n* = 3). (b) The tiller buds of KN199 and three independent *TaD27*-RNAi-transgenic plants in hydroponic culture with or without 5.0 μM GR24. (c) The tiller buds of wild-type control (KN199) and three independent *TaD27-B*-OE-transgenic plants in hydroponic culture with or without 3.0 μM T is108. Bars = 1 mm.

IAA and *SAUR* family genes were down-regulated in *TaD27*-RNAi plants. Two *AUXIN RESPONSE FACTOR* (*ARF*) genes were down-regulated (Figure 7a; Table S5). Thus, it is likely that *TaD27s* regulate axillary bud outgrowth through auxin signalling. In addition, genes related to other phytohormones were identified in our DEGs (cytokines: CKX2, CKX4CKX7; ABA: CYP707A7, CYP707A5; gibberellin: GA2OX1, GA3OX2; ethylene: ERFs), suggesting that SLs signalling pathways might crosstalk with the signalling and biosynthesis of other phytohormones (Table S5).

Several subfamilies of TFs are reported to play critical roles in the regulation of branching (tillering). For example, CUC1, CUC2 and CUC3, belonging to NAC domain TFs, redundantly regulate the initiation of AMs, in addition to initiating the SAM and establishing organs in *Arabidopsis* (Laufs *et al.*, 2004). These TFs can directly suppress the expression of *D14*, enhance the axillary bud outgrowth and subsequent tillering via SLs signalling (Guo *et al.*, 2013). In our data, 369 putative TFs were identified in the DEGs, and the most abundant TF families were the ERF, MYB, bHLH, NAC and WRKY families (Figure 7b; Table S6). This suggested that TFs might function in axillary meristem initiation and bud growth in wheat as they do in *Arabidopsis* and rice.

Coexpression network analysis was performed as an independent way to validate the functions of the *TaD27* genes. The correlations between the expression profiles of the DEGs and *TaD27-B* were calculated. A gene network of 451 DEGs was constructed in the current study with Cytoscape (*P*-value ≤0.05 and cor ≥0.9). Functional enrichment shows that 451 DEGs were associated with various biological processes. Especially, 16 DEGs were involved in hormone signalling pathway and 21 DEGs encode the TFs, implying that those genes might participate in the regulation of tiller bud number in wheat (Figure 7; Table S7). Further study is required to investigate their functions in wheat tillering in the future.

Discussion

Conservation of D27 function among rice, wheat and *Arabidopsis*

The shoot branching is generated at three stages, the initiation of the AM, bud development and the outgrowth of axillary buds. Recent molecular and genetic studies have demonstrated that D27 proteins regulate axillary bud outgrowth through the MAX/RMS/D pathway in *Arabidopsis* and rice (Beveridge and Kyozuka, 2010; Lin *et al.*, 2009). In our study, the overexpression of *TaD27-B* resulted in rescuing the tiller phenotype of the *Arabidopsis Atd27* mutants (Figure S2). Compared with the wild-type KN199, the *TaD27*-RNAi wheat plants displayed increased tiller numbers; in contrast, the *TaD27-B*-OE wheat plants showed reduced tiller numbers (Figures 3 and 5). The statistical analyses at the jointing stage confirmed that *TaD27-B* regulates axillary bud number. RNA-Seq analysis showed the expression levels of *TaD27, TaMAX1, TaD3, TaD14* and *TaD53* were markedly changed (Figure 6a). This suggested that the MAX/RMS/D pathway might participate in the regulation of tillering in wheat, and they might have well conserved mechanisms controlling shoot branching in different species such as rice, wheat and *Arabidopsis*. The expression levels of *TaD27-A* and *TaD27-D* were also significantly decreased in *TaD27*-RNAi wheat plants (Figure 3h). Considering that three homologous TaD27s have high sequence similarity (>95%), we speculate that *TaD27-A* and *TaD27-D* might have the same biological function as TaD27-B in regulating tiller number.

(a)

(b)

(c)

Top 20 of pathway enrichment

However, subtle phenotype differences were observed in *TaD27*-RNAi wheat plants compared with *d27* mutants of rice and Arabidopsis. SLs suppress axillary bud outgrowth by

regulating *Teosinte branched1*(*TB1*) gene in *Arabidopsis* and rice, and the plant height was also affected in both plant species (Aguilar-Martínez *et al.*, 2017; Minakuchi *et al.*, 2010). Here,
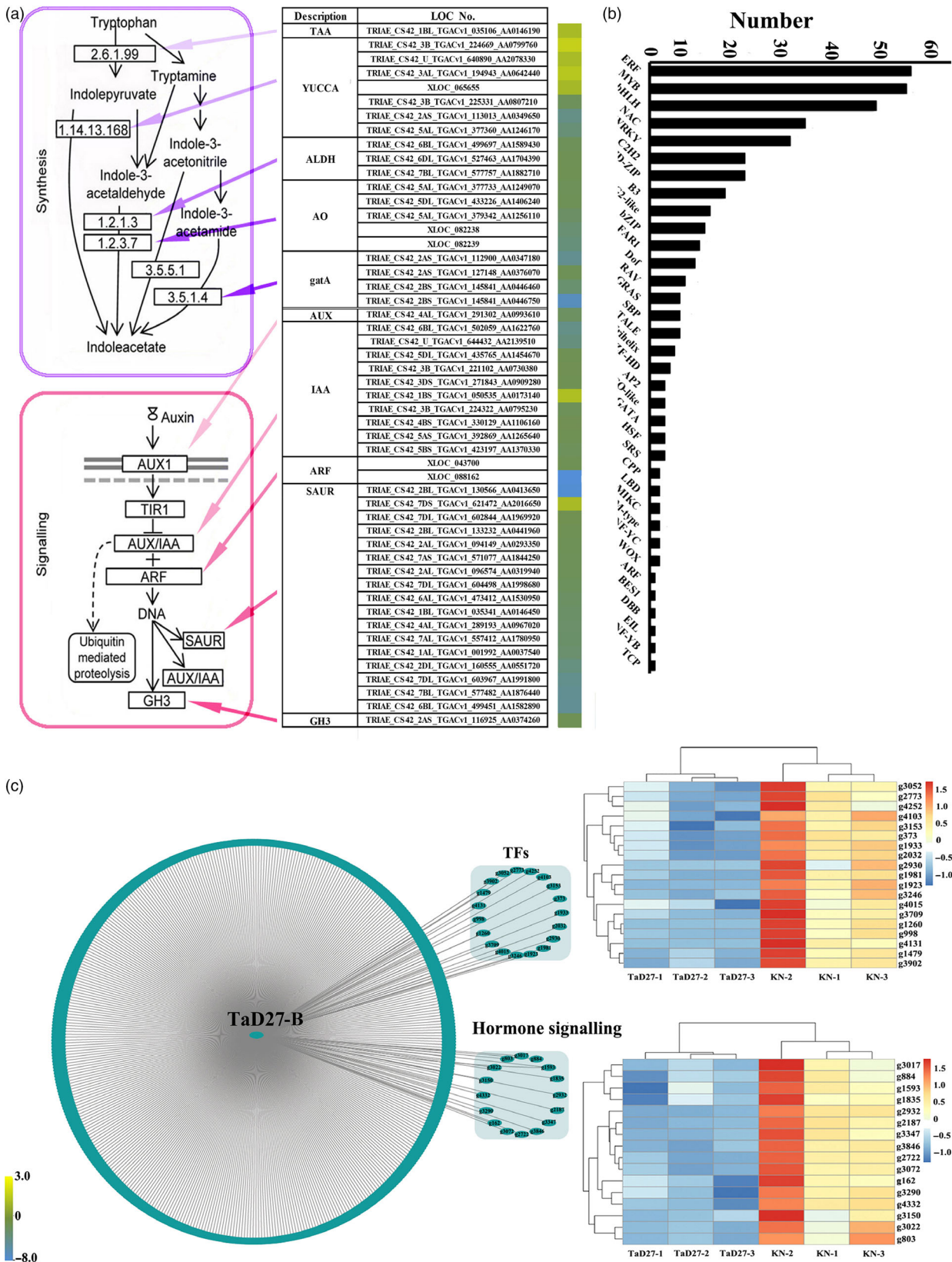
Figure 7 (a) Auxin biosynthesis and signalling pathway-related genes in the DEGs. The colour scale indicates the relative transcript abundance determined by log$_2$ ratios (*TaD27*-RNAi *vs* KN199). (b) Distribution of TFs in the DEGs. (c) Coexpression network of TaD27-B with the DEGs displaying the highly connected groups. The network was constructed using Cytoscape. The transcript IDs corresponding to the numbers are shown in Table S7. *TaD27*-1, *TaD27*-2 and *TaD27*-3 indicate three *TaD27*-RNAi axillary bud samples, respectively. KN-1, KN-2 and KN-3 indicate three axillary bud samples of the wild-type KN199, respectively.

although the tiller number was obviously changed, plant height was not significantly changed in *TaD27*-RNAi or *TaD27-B*-OE plants (Figures 3h and 4h). Exogenous application of GR24 had no effect on the height of *TaD27*-RNAi and wild-type plants (Figure S4). Moreover, in our RNA-seq data, the expression levels of *TaTB1* genes (TRIAE_CS42_4AL_TGACv1_290526_AA0986 290, TRIAE_CS42_4BS_TGACv1_327850_AA1076210 and TRI AE_CS42_4DS_TGACv1_361050_AA1159720) had no significant change. It suggested the TaD27 proteins may not be involved in the regulation of plant height in wheat. Of course, although the gene-specific primers of *TaD27*s were designed and the sequence of the inserted cDNA fragment was confirmed by Sanger sequence when constructing the *TaD27*-RNAi vectors, we cannot rule out the possibility that the knock-down of *TaD27*s was not effective enough to interfere with plant height.

Roles of strigolactones in regulating wheat tillering

Strigolactones are important phytohormones which can inhibit axillary bud outgrowth in various plant species (Gomezroldan *et al.*, 2008; Umehara *et al.*, 2008). The reduction of SLs synthesis, perception and signalling leads to the fast outgrowth of axillary buds (Domagalska and Leyser, 2011; Ruyter-Spira *et al.*, 2013). In our study, *TaD27*-RNAi wheat plants had more tillers and *TaD27-B*-OE wheat plants had fewer tillers. Germination bioassay of *Orobanche* and exogenous supplementation of GR24 or TIS108 confirmed *TaD27-B* plays a role in SLs biosynthesis in wheat (Figure 4). RNA-seq data showed the genes involved in SLs synthesis and transduction were suppressed in *TaD27*-RNAi-transgenic plants (Figure 6a). Thus, the results suggested that *TaD27-B* genes might play key roles in regulating wheat tiller number by affecting SLs synthesis.

The interactions between SLs and auxins in regulating shoot branching have been investigated previously (Liang *et al.*, 2010; Ward *et al.*, 2013). There are two models for bud suppression by SLs. One model is the secondary messenger hypothesis, which proposes that the synthesis of SLs is regulated by the auxin within the bud, acts as the second messengers to regulate branching (Brewer *et al.*, 2009, 2015; Tanaka *et al.*, 2006). An alternative model is the PAT hypothesis, which proposes that SLs act systemically by modulating the transport of auxin (Bennett and Iossa, 2006; Prusinkiewicz *et al.*, 2009) . In *Arabidopsis*, rice and pea, SLs modulate the redistribution of growth in the shoot by swiftly regulating auxin transport, which supports the PAT hypothesis (Bennett and Leyser, 2014; Crawford *et al.*, 2010; Lin *et al.*, 2009; Shinohara *et al.*, 2013). Our transcriptomic data showed that multiple biological processes were affected by *TaD27* knock-down and that auxin synthesis and signalling-related genes were abundant among the DEGs, such as *SAUR*, *IAA* and *ARF* genes (Figure 7a). However, no genes encoding PIN1s were identified in our DEGs. Virus-induced gene silencing of the *TaPIN1* genes resulted in up to a 26% reduction in plant height (Singh *et al.*, 2018). But there were no significant changes in the height of *TaD27*-RNAi plants (Figure 3h), suggesting that knock-down of *TaD27*s might have no effect on auxin polar transport by TaPIN1s in *TaD27*-RNAi-transgenic plants. Moreover, 16 genes involved in hormone signalling pathways were shown to have close relationships with *TaD27-B* by Cytoscape analysis, including two auxin-responsive genes (TRIAE_CS42_2BL_TGAC-v1_133232_AA0441960 and TRIAE_CS42_U_TGACv1_644 432_AA2139510) (Figure 7c; Table S7). Thus, it is possible that TaD27-B regulates tiller bud outgrowth through auxin signalling in wheat, at least in part.

Experimental procedures

Plant materials and growing conditions

The wheat grains were sowed on October 15 in 2017 and harvested on June 18 in 2018 at the Experimental Station of Shandong Agricultural University, Tai'an, Shandong province, China (36°09′N, 117°09′E; 128 m above sea level). The soil is classified as the sandy loam soil. For phenotype investigation, transgenic wheat and wild-type plants were grown under natural conditions. Weather data and soil condition were listed in Table S1. To facilitate the statistics of tiller number, each experimental line was sowed with 25 cm in-row spacing and 12.5 cm plant-to-plant spacing. GR24 and TIS108 were purchased from StrigoLab (Turin, Italy). For 5.0 μM and 3.0 μM TIS108 treatment, the germinated wheat seeds were placed on a nylon net floating on the hydroponic solution in an illumination incubator.

The *Atd27* mutant was isolated from the GABI-Kat collection (CS761234) and obtained from the European *Arabidopsis* Stock Centre. The wild-type *Arabidopsis* (ecotype C24) and *Atd27* mutant plants were cultivated as described by Wang *et al.* (2006).

DNA isolation, RNA extraction and qRT-PCR Analysis

The CTAB method was used to extract the genomic DNA from wheat leaves (Saghai-Maroof *et al.*, 1984). Total RNA was first isolated from different wheat (cv. Kenong199) tissues with the TRIzol reagent (CWBiotech, Beijing, China) then was purified by the treatment with RNase-free DNaseI (CWBiotech, Beijing, China). The transcript levels of *TaD27-A*, *TaD27-B* and *TaD27-D* in various wheat (cv. Kenong199) organs were analysed by qRT-PCR. For qRT-PCR, the first-strand cDNAs were synthesized by 2 μg of RNA per sample using TransScript One-Step gDNA Removal and cDNA Synthesis SuperMix (TransGen, Beijing, China). The qRT-PCR amplifications were performed as described by Zhao *et al.* (2016). Amplification of *TaActin* was used as an internal control for data normalization. Those experiments were independently replicated for three times under identical conditions. The results were displayed as the mean ± standard errors of three individual experiments. All primers were listed in Table S2.

In situ hybridization

Wheat tissues were first fixed in 4% paraformaldehyde overnight at 4 °C, then embedded in surgipath paraplast (Leica Route, Richmond, IL) and finally sectioned at 8 μm. To detect the expression patterns of *TaD27-B*, the 150-600-bp region (counted from the start codon) of *TaD27-B* was amplified and used as the template. Antisense and sense probes were labelled *in vitro* with a digoxigenin RNA labelling kit (Sigma-Aldrich, Mannheim, Germany). The hybridization and the detection of hybridized signals were carried out as described by Wang *et al.* (2006).

Vector construction and plant transformation

For subcellular localization, we transferred a *35S::TaD27-B-GFP* construct into the pROKII vector and then introduced it into *Agrobacterium tumefaciens* GV3101. *35S::TaD27-B-GFP* was transferred into the protoplasts of *Arabidopsis* leaf. The chlorophyll autofluorescence and TaD27-B-GFP signal were detected by the Leica confocal microscope. *Arabidopsis Atd27* mutant plants were transformed using the vacuum infiltration method described by Clough and Bent (1998). The transgenic *Arabidopsis* plants

were screened in media with kanamycin (50 g/mL) and further verified by RT-PCR.

For wheat transformation, *TaD27-B* full length cDNA was inserted into the Gateway-compatible OE vector PC186 (*pUbi*::*GW_{OE}*::*Nos*). The 243-580-bp region (counted from the start codon) of *TaD27-B*, which was identified to be specific in wheat genome and conserved in *TaD27-A* and *TaD27-D*, was cloned into the RNAi vector PC336. The PCR primers were listed in Table S2. The *TaD27*-RNAi and *TaD27-B*-OE vectors were introduced into hexaploid wheat (cv. Kenong199) via Agrobacterium-mediated transformation as described by Tao *et al.* (2011). PCR, herbicide (glufosinate) spraying and a QuickStix Kit for *bar* were used to verify the positive transgenic plants.

Germination assay

Strigolactones were extracted from the root tissues of wild type, *TaD27*-RNAi and *TaD27-B*-OE as reported previously (Ma *et al.*, 2013). The germination assay using *Orobanche aegyptiaca* seeds was performed as described previously (Sugimoto and Ueyama, 2008). Five micromolar GR24 solution and deionized water were used as positive and negative controls, respectively. The germinated *Orobanche* seeds were counted after 10 days using a stereomicroscope. All experiments were repeated for three times, and the data represent mean ± standard errors.

Library construction, sequencing and data analysis

Total RNAs were extracted with a RNeasy Plus Micro kit (Qiagen, Valencia, CA). The products were sequenced using an Illumina HiSeq™ 2500 by Gene Denovo Biotechnology Co. (Guangzhou, China). The RNA-seq data were obtained from three biological replicates and deposited in NCBI GEO (GSE124767). The filtered clean reads were mapped to the wheat reference genome and genes (http://plants.ensembl.org/Triticum_aestivum/Info/Index).

FPKM values can represent the relative expression levels (Mortazavi *et al.*, 2008). The differential expression analysis of the two samples was performed using the DESeq R package (1.10.1). To control the false discovery rate (FDR), the resulting *P*-values were adjusted using Benjamini and Hochberg's approach. DEGs were identified between each comparison with |fold change| ≥1.0 and FDR < 0.05. Then, KEGG pathway and GO analyses were carried out (Moriya *et al.*, 2007; Young *et al.*, 2010).

Coexpression network construction

To further identify genes those were associated with the regulation of tiller number, the correlation coefficient of the DEGs between *TaD27-B* was calculated using R (R Studio, version 1.1.383) (Table S5). The correlation coefficient value ranges from −1 to +1, the value −1 indicated a prefect negative correlation, and +1 represented a prefect positive correlation. 451 DEGs were identified with *P*-value ≤0.05 and cor ≥0.9. Subsequently, the coexpression network was reconstructed with Cytoscape (version 3.6.0).

Conflict of interest

The authors declare that the research was conducted in the absence of any commercial or financial relationships that could be construed as a potential conflict of interest.

Author contributions

WF and ZhXS planned and designed the research. ZhB, WTT, MSS and BXM performed experiments. WF and JDJ analysed data. WF, ZhXS and SN wrote the manuscript.

References

Aguilar-Martínez, J.A., Poza-Carrión, C. and Cubas, P. (2017) *Arabidopsis BRANCHED1* acts as an integrator of branching signals within axillary buds. *Plant Cell* **19**, 458–472.

Albabili, S. and Bouwmeester, H.J. (2015) Strigolactones, a novel carotenoid-derived plant hormone. *Annu. Rev. Plant Biol.* **66**, 161–186.

Alder, A. and Al-Babili, S. (2012) The path from β-carotene to carlactone, a strigolactone-like plant hormone. *Science* **335**, 1348–1351.

Arite, T., Iwata, H., Ohshima, K., Maekawa, M., Nakajima, M., Kojima, M., Sakakibara, H. *et al.* (2010) *DWARF10*, an *RMS1/MAX4/DAD1* ortholog, controls lateral bud outgrowth in rice. *Plant J.* **51**, 1019–1029.

Babb, S. and Muehlbauer, G.J. (2003) Genetic and morphological characterization of the barley *uniculm2* (*cul2*) mutant. *Theor. Appl. Genet.* **106**, 846–857.

Bennett, J. and Iossa, E. (2006) Building and managing facilities for public services. *J. Pub. Econ.* **90**, 2143–2160.

Bennett, T. and Leyser, O. (2014) Strigolactone signalling: standing on the shoulders of DWARFs. *Curr. Opin. Plant Biol.* **22**, 7–13.

Beveridge, C.A. and Kyozuka, J. (2010) New genes in the strigolactone-related shoot branching pathway. *Curr. Opin. Plant Biol.* **13**, 34–39.

Booker, J., Sieberer, T., Wright, W., Williamson, L., Willett, B., Stirnberg, P., Turnbull, C. *et al.* (2005) *MAX1* encodes a cytochrome P450 family member that acts downstream of *MAX3/4* to produce a carotenoid-derived branch-inhibiting hormone. *Dev. Cell* **8**, 443–449.

Brewer, P.B., Dun, E.A., Ferguson, B.J., Rameau, C. and Beveridge, C.A. (2009) Strigolactone acts downstream of auxin to regulate bud outgrowth in pea and *Arabidopsis*. *Plant Physiol.* **150**, 482–493.

Brewer, P.B., Dun, E.A., Gui, R., Mason, M.G. and Beveridge, C.A. (2015) Strigolactone inhibition of branching independent of polar auxin transport. *Plant Physiol.* **168**, 1820.

Clough, S.J. and Bent, A.F. (1998) Floral dip: a simplified method for Agrobacterium-mediated transformation of *Arabidopsis* thaliana. *Plant J.* **16**, 735–743.

Conn, C.E., Bythell-Douglas, R., Neumann, D., Yoshida, S., Whittington, B., Westwood, J.H., Shirasu, K. *et al.* (2015) Plant evolution of strigolactone perception enabled host detection in parasitic plants. *Science* **349**, 540.

Crawford, S., Shinohara, N.T., Williamson, L., George, G., Hepworth, J., Muller, D., Domagalska, M.A. *et al.* (2010) Strigolactones enhance competition between shoot branches by dampening auxin transport. *Development* **137**, 2905.

Dabbert, T., Okagaki, R.J., Cho, S., Boddu, J. and Muehlbauer, G.J. (2009) Thegenetics of barley low-tillering mutants: *absent lower laterals* (*als*). *Theor. Appl. Genet.* **118**, 1351–1360.

Dabbert, T., Okagaki, R.J., Cho, S., Heinen, S., Boddu, J. and Muehlbauer, G.J. (2010) The genetics of barley low-tillering mutants: *low number of tillers-1* (*lnt1*). *Theor. Appl. Genet.* **121**, 705–715.

Domagalska, M.A. and Leyser, O. (2011) Signal integration in the control of shoot branching. *Nat. Rev. Mol. Cell Biol.* **12**, 211–221.

Gomezroldan, V., Fermas, S., Brewer, P.B., Puechpagès, V., Dun, E.A., Pillot, J.P., Letisse, F. *et al.* (2008) Strigolactone inhibition of shoot branching. *Nature* **455**, 189–194.

Guo, S., Xu, Y., Liu, H., Mao, Z., Zhang, C., Ma, Y., Zhang, Q. *et al.* (2013) The interaction between OsMADS57 and OsTB1 modulates rice tillering via DWARF14. *Nat. Commun.* **4**, 1566.

Hagen, G. and Guilfoyle, T. (2002) Auxin-responsive gene expression: genes, promoters and regulatory factors. *Plant Mol. Biol.* **49**, 373–385.

Ito, S., Umehara, M., Hanada, A., Kitahata, N., Hayase, H., Yamaguchi, S. and Asami, T. (2011) Effects of triazole derivatives on strigolactone levels and growth retardation in rice. *PLoS One* **6**, e21723.

Jia, K.P., Baz, L. and Albabili, S. (2017) From carotenoids to strigolactones. *J. Exp. Bot.* **69**, 2189–2204.

Jiang, L., Liu, X., Xiong, G., Liu, H., Chen, F., Wang, L., Meng, X. *et al.* (2013) DWARF 53 acts as a repressor of strigolactone signalling in rice. *Nature* **504**, 401.

Laufs, P., Peaucelle, A., Morin, H. and Traas, J. (2004) MicroRNA regulation of the *CUC* genes is required for boundary size control in *Arabidopsis* meristems. *Development* **19**, 4311–4322.

Liang, J., Zhao, L., Challis, R. and Leyser, O. (2010) Strigolactone regulation of shoot branching in chrysanthemum (*Dendranthema grandiflorum*). *J. Exp. Bot.* **61**, 3069.

Lin, H., Wang, R., Qian, Q., Yan, M., Meng, X., Fu, Z., Yan, C. *et al.* (2009) DWARF27, an iron-containing protein required for the biosynthesis of strigolactones, regulates rice tiller bud outgrowth. *Plant Cell* **21**, 1512–1525.

Lópezráez, J.A., Matusova, R., Cardoso, C., Jamil, M., Charnikhova, T., Kohlen, W., Ruyterspira, C. *et al.* (2010) Strigolactones: ecological significance and use as a target for parasitic plant control. *Pest Manag. Sci.* **65**, 471–477.

Ma, Y., Jia, J., An, Y., Wang, Z. and Mao, J. (2013) Potential of some hybrid maize lines to induce germination of sunflower broomrape. *Crop Sci.* **53**, 260–270.

Mangnus, E.M., Dommerholt, F.J., De Jong, R.L. and Zwanenburg, B. (1992) Improved synthesis of strigol analog GR24 and evaluation of the biological activity of its diastereomers. *J. Agric. Food Chem.* **40**, 1230–1235.

Mascher, M., Jost, M., Kuon, J.E., Himmelbach, A., Aßfalg, A., Beier, S., Scholz, U. *et al.* (2014) Mapping-by-sequencing accelerates forward genetics in barley. *Genome Biol.* **15**, R78.

Mcsteen, P. and Leyser, O. (2005) Shoot branching. *Annu. Rev. Plant Biol.* **56**, 353–374.

Minakuchi, K., Kameoka, H., Yasuno, N., Umehara, M., Luo, L., Kobayashi, K., Hanada, A. *et al.* (2010) *FINE CULM1* (*FC1*) works downstream of strigolactones to inhibit the outgrowth of axillary buds in rice. *Plant Cell Physiol.* **51**, 1127–1135.

Moriya, Y., Itoh, M., Okuda, S., Yoshizawa, A.C. and Kanehisa, M. (2007) KAAS: an automatic genome annotation and pathway reconstruction server. *Nucleic Acids Res.* **35**, 182–185.

Mortazavi, A., Williams, B.A., McCue, K., Schaeffer, L. and Wold, B. (2008) Mapping and quantifying mammalian transcriptomes by RNA-Seq. *Nat. Methods* **5**, 621–628.

Prusinkiewicz, P., Crawford, S., Smith, R.S., Ljung, K., Bennett, T., Ongaro, V., Leyser, O. *et al.* (2009) Control of bud activation by an auxin transport switch. *Proc. Natl Acad. Sci. USA* **106**, 17431–17436.

Ruyter-Spira, C., Al-Babili, S., Krol, S.V.D. and Bouwmeester, H. (2013) The biology of strigolactones. *Trends Plant Sci.* **18**, 72–83.

Saghai-Maroof, M.A., Soliman, K.M., Jorgensen, R.A. and Allard, R.W. (1984) Ribosomal DNA spacer-length polymorphisms in barley: mendelian inheritance, chromosomal location, and population dynamics. *Proc. Natl Acad. Sci. USA* **81**, 8014–8018.

Shimizu-Sato, S. and Mori, H. (2001) Control of outgrowth and dormancy in axillary buds. *Plant Physiol.* **127**, 1405–1413.

Shinohara, N., Taylor, C. and Leyser, O. (2013) Strigolactone can promote or inhibit shootbranching by triggering rapid depletion of the auxin efflux protein PIN1 from the plasma membrane. *PLoS Biol.* **11**, e1001474.

Singh, K., Singh, J., Jindal, S., Sidhu, G., Dhaliwal, A. and Gill, K. (2018) Structural and functional evolution of an auxin efflux carrier PIN1 and its functional characterization in common wheat. *Funct. Integr. Genomics* 1–13.

Soundappan, I., Bennett, T., Morffy, N., Liang, Y., Stanga, J.P., Abbas, A., Leyser, O. *et al.* (2015) SMAX1-LIKE/D53 family members enable distinct MAX2-dependent responses to strigolactones and karrikins in *Arabidopsis*. *Plant Cell* **27**, 3143.

Sugimoto, Y. and Ueyama, T. (2008) Production of (+)-5-deoxystrigol by *Lotus japonicus* root culture. *Phytochemistry* **69**, 212–217.

Tanaka, Y., Sano, T., Tamaoki, M., Nakajima, N., Kondo, N. and Hasezawa, S. (2006) Cytokinin and auxin inhibit abscisic acid-induced stomatal closure by enhancing ethylene production in *Arabidopsis*. *J. Exp. Bot.* **57**, 2259–2266.

Tao, L.L., Yin, G.X., Du, L.P., Shi, Z.Y., She, M.Y., Xu, H.J. and Ye, X.G. (2011) Improvement of plant regeneration from immature embryos of wheat infected by *Agrobacterium tumefaciens*. *Agric. Sci. China* **10**, 317–326.

Tavakol, E., Okagaki, R., Verderio, G., Shariati, J.V., Hussien, A., Bilgic, H., Scanlon, M.J. *et al.* (2015) The barley *Uniculme4* gene encodes a BLADE-ON-PETIOLE-like protein that controls tillering and leaf patterning. *Plant Physiol.* **168**, 164–174.

Umehara, M., Hanada, A., Yoshida, S., Akiyama, K., Arite, T., Takedakamiya, N., Magome, H. *et al.* (2008) Inhibition of shoot branching by new terpenoid plant hormones. *Nature* **455**, 195–200.

Wang, F., Huo, S.N., Guo, J. and Zhang, X.S. (2006) Wheat D-type cyclin *Triae; CYCD2; 1* regulate development of transgenic *Arabidopsis* plants. *Planta* **224**, 1129–1140.

Wang, X.M., Liang, Y.Y., Ling, L.I., Gong, C.W., Wang, H.P., Huang, X.X., Shuang-Cheng, L.I. *et al.* (2015) *OsMAX1a* and *OsMAX1e*, involved in the biosynthesis of strigolactones, regulate rice tillering. *Chin. J. Rice Sci.* **69**, 168–173.

Ward, S.P., Salmon, J., Hanley, S.J., Karp, A. and Leyser, O. (2013) Using Arabidopsis to study shoot branching in biomass willow. *Plant Physiol.* **162**, 800–811.

Waters, M.T., Brewer, P.B., Bussell, J.D., Smith, S.M. and Beveridge, C.A. (2012) The Arabidopsis ortholog of rice DWARF27 acts upstream of MAX1 in the control of plant development by strigolactones. *Plant Physiol.* **159**, 1073–1085.

Waters, M.T., Gutjahr, C., Bennett, T. and Nelson, D.C. (2017) Strigolactone signaling and evolution. *Annu. Rev. Plant Biol.* **68**, 291.

Young, M.D., Wakefield, M.J., Smyth, G.K. and Oshlack, A. (2010) Gene ontology analysis for RNA-seq: accounting for selection bias. *Genome Biol.* **11**, R14–R14.

Zhang, Y., Dijk, A.D.J.V., Scaffidi, A., Flematti, G.R., Hofmann, M., Charnikhova, T., Verstappen, F. *et al.* (2014) Rice cytochrome P450 MAX1 homologs catalyze distinct steps in strigolactone biosynthesis. *Nat. Chem. Biol.* **10**, 1028.

Zhao, X.Y., Hong, P., Wu, J.Y., Chen, X.B., Ye, X.G., Pan, Y.Y., Wang, J. *et al.* (2016) The tae-miR408-mediated Control of *TaTOC1* gene transcription is required for the regulation of heading time in wheat (*Triticum aestivum* L.). *Plant Physiol.* **170**, 1578.

Zhou, F., Lin, Q., Zhu, L., Ren, Y., Zhou, K., Shabek, N., Wu, F. *et al.* (2013) D14-SCFD3-dependent degradation of D53 regulates strigolactone signalling. *Nature* **504**, 406.

Zou, J., Chen, Z., Zhang, S., Zhang, W., Jiang, G., Zhao, X., Zhai, W. *et al.* (2005) Characterizations and fine mapping of a mutant gene for high tillering and dwarf in rice (*Oryza sativa* L.). *Planta* **222**, 604–612.

Supporting information

Additional supporting information may be found online in the Supporting Information section at the end of the article.

Figure S1 Alignment of TaD27 homologues with OsD27 and AtD27.

Figure S2 Genetic complementation of Arabidopsis *d27* mutant with 35S::*TaD27*.

Figure S3 Identification of transgenic wheat.

Figure S4 (a) Seedlings of 3-week-old KN199 and three independent *TaD27*-RNAi transgenic lines in the hydroponic culture. Bar = 5 cm. (b) Column diagram showing statistical analysis of plant height (Student's *t*-test, $P < 0.01$, $n = 30$).

Figure S5 Validation of RNA-seq results by RT-qPCR.
Table S1 Soil condition, monthly rainfall and mean temperature (°C) recorded during the period of winter wheat growth (October to next June).
Table S2 Lists of the primers.
Table S3 Genes expressed in all samples.

Table S4 Lists of the DEGs.
Table S5 Lists of TF families in DEGs.
Table S6 Lists of genes involved in hormones in DEGs.
Table S7 The transcript IDs corresponding to the numbers in Cytoscape analysis.